Hybrid solar-driven hydrogen generation by sorption enhanced–chemical looping and hydrocarbon reforming coupled with carbon capture and Rankine cycle.

Linus Onwuemezie, Hamidreza Gohari Darabkhani*, Mohammad Moghimi Ardekani

Department of Engineering, School of Digital, Technologies and Arts (DTA), Staffordshire University, Stoke-on-Trent, ST4 2DE, UK

** Corresponding Author email: h.g.darabkhani@staffs.ac.uk*

ABSTRACT

Hydrogen (H_2) production from fossil fuels using Hydrocarbon Reforming Methods (HRM) accounts for nearly 95% of Global H_2 production. Unlike hybrid CL-SR systems, the Integrated Solar-Driven Sorption Enhanced–Chemical Looping of Hydrocarbon Reforming (SE-CL-HR) utilises solar thermal energy from the CSP system to drive the endothermic decomposition of feedstocks. Furthermore, the simulated hybrid systems utilise recovered heat to generate electricity, reuse of by-product CO_2 for more syngas production and CO_2 capture by a reaction of CaO to form $CaCO_3$. This work focused on modelling and simulating hybrid CSP systems and SE-CL-HR plants with HTF output temperatures between 750 - 1050°C. In this study, SAM and MATLAB are used to develop the CSP system. While the CSP result saved in the MATLAB workspace gets exported to Simulink to feed SE-CL-SMR, SE-CL-POX and SE-CL-ATR Aspen plus models. The integrated system is fed with CH_4 as the working fluid of the solar furnace. Stoichiometric and Gibbs free-energy minimisation were employed to investigate the effect of operating parameters. The output of the integrated system shows ≥ 9.5% exergy efficiency in comparison to conventional HRM. In addition, CO_2 capture by CaO and high-pH water (Ca, Mg, Na^+, O_2, OH^- and Cl^-) to produce $CaCO_3$, $MgCO_3$ and other valuable products was also investigated in a process simulation. The research results revealed that for 8.1 $tons/hr$ of CH_4 and 277.1 $tons/hr$ H_2O (steam) flowrates, 62 $tons/hr$ of H_2 can be generated and 338.5 $tons/hr$ of CO_2 emission can be reused and captured by the adoption of these new innovative technologies.

Keywords:
Concentrating Solar Power (CSP)
Steam Methane Reforming (SMR)
Partial Oxidation of Methane (POM)
Autothermal Reforming (ATR)
Sorption Enhanced–Chemical Looping (SE-CL)
Rankine Cycle (RC)

Nomenclature

Abbreviations and Symbols

%	Percentage
°C	Degrees Celsius
ΔH	Enthalpy
$m\mu$	Millimicron
n	Efficiency
μm	Micron
wt.%	Percentage by weight
ASU	Air separation unit
ATR	Autothermal reforming
By-CO_2	Carbon dioxide by-product
CCUS	Carbon capture and utilisation and storage
CL-SR	Chemical looping steam reforming
CO_2e	Carbon emission equivalent
CSP	Concentrating Solar Power
CSPS	Concentrating Solar Power System
DNI	Direct normal irradiance
HNDP	Hybrid microwave discharge plasma
HR	Hydrocarbon Reforming
HTF	Heat Transfer Fluids
HTS	High-temperature shift
HEX	Heat exchangers
HX	Heat exchangers
kg/hr	Kilo gram per hour
$kmol/hr$	Kilo mole per hour
kW	Kilowatt
LTS	Low-temperature shift
m^2	square metre
m/s	Metre per second
MENA	The Middle East and North Africa
MPS	Microwave plasma source
MW	Megawatt
NREL	National Renewable Energy Laboratory
PMD	Plasma microwave discharge
PMDP	Plasma microwave discharge process
POM	Partial oxidation of methane
PR	Plasma reforming
PSA	Pressure swing adsorption
S/C	Steam carbon ratio
SAM	System Advisor Model
SE-CL	Sorption Enhanced–Chemical Looping
SMR	Steam methane reforming
WGS	Water gas shift
W/m^2	Watt per square metre

1.0 Introduction

The Global energy crisis and greenhouse emissions as a result of fast-growing energy consumption remain the biggest challenges facing humanity. Currently, Global energy demand is met by fossil liquid and gaseous fuels due to their availability and convenience of use [1]. For this reason, the environmental impact of greenhouse emissions continues to increase as the combustion of fossil fuels without carbon capturing and storage releases carbon emissions into the atmosphere. Hydrogen (H_2) fuel from renewable and fossil fuels with carbon capture and utilisation and storage (CCUS) has been viewed as a major replacement for fossil fuels combustion to produce energy. In contrast to renewable sources of H_2 production, fossil fuels-based method account for 95% of Global H_2 production [2]. At present, H_2 production from hydrocarbon reforming such as steam methane reforming (SMR), partial oxidation (POX) reforming, autothermal reforming (ATR) and plasma reforming are well-established technologies [2]. While sorption enhanced–chemical looping (SE-CL) is an emerging fossil-based method of extracting H_2 from other elements [2]. Each of these technologies uses light hydrocarbon which is fed to the reformer and combustor in the presence of oxidising agents (H_2O and O_2) and catalyst to produce H_2 and other syngas (CO, CO_2 and C_2H_2). The above systems of producing H_2 requires water gas shift (WGS) and purification units to increase H_2 yield and separate H_2 from other by-products. The introduction of a catalyst in the reformer promotes syngas concentration at lower activation energy [3]. An external heat source is supplied to drive the endothermic reforming and combustion reactions that decompose feeds into H_2 and other synthetic gas. However, the lack of thermal energy from non-polluting sources to drive the endothermic reactions, recovery, and capture of CO_2 by-product remain unsolved issues with these technologies. Thus, efficiency improvement that allows the use of wasted thermal energy to drive downstream reactions and generate electricity in a Rankine cycle can improve the overall efficiency of these systems.

Steam methane reforming (SMR) is the most advanced and one of the cheapest H_2 production technology. In SMR system, a mixture of methane (CH_4) after sulphur removal and steam from the vaporiser is fed to the reformer. The reformer with the presence of catalysts like a commercial nickel-alumina (Ni/Al_2O_3) produces synthetic gas at an operating temperature ≥ 800°C [4]. The introduction of WGS which is made up of high-temperature shift (HTS) and low-temperature shift (LTS) converts CO to CO_2 and increases the H_2 concentration rate. While upstream and downstream heat exchangers (HEX) before and after the first shift reactor allows proper conditioning of the reactant temperature. A pressure swing adsorption (PSA) separate H_2 from other syngas at high purity [3]. Despite the advantages of SMR such as being the most widespread and cheaper than competing technologies for H_2 production, *Bareiß, et al.* [5] reported that 8.8kg of CO_2 is generated for every 1kg of H_2 produced from fossil fuels. In addition, *Spallina, et al.* [6] mentioned that the high cost of H_2 purification unit in contrast to other units increases the complexity of the system (SMR). Therefore, incorporating solar energy or electricity to drive the endothermic reactions of feeds and carbon capture units can decrease the overall carbon footprints of SMR system. For these reasons, a plasma microwave discharge (PMD) process was developed to mitigate carbon emission associated with reforming of CH_4 and H_2O_{gas} (steam) in a H_2 generation plant. Plasma reforming (PR) process which involves the passage of pure gaseous hydrocarbon like CH_4 into plasma microwave discharge to produce carbon soot and H_2 uses electricity [7]. Compactness, low density, high conversion efficiency because of a high degree of ionisation, fuel diversity, absence of catalyst, and quick response time are some of the advantages of the plasma reforming process of H_2 generation. Nevertheless, high electricity dependency which increase H_2 selling price, difficulties in handling high operating pressure and temperature, and electrode erosion are reported as drawbacks of the system [8]. A short while ago, a co-production of H_2 by hybrid microwave discharge plasma (HMDP) and SMR processes with CH_4, CO_2 and H_2O_{gas} as feedstocks were investigated by *Czylkowski, et al.* [9]. It was found that an increase of CO_2 flowrate accelerates the rate of unprocessed CO_2 and decreases the H_2 volume concentration at the microwave plasma source (MPS) outlet. The investigated result shows that H_2 yield was lower because of the influence of CO_2 and minimal percentage of unprocessed CH_4. Therefore, use of non-polluting sources of thermal energy rather than electricity to drive endothermic reforming and efficiency improvement techniques as mentioned above are urgently needed. Eqs (1 - 4) are desulphurisation, chemical reactions of SMR, WGS, and Net SMR with WGS processes of H_2 generation. While Eq 5 represents the chemical reaction of integrated microwave plasma, steam methane and CO_2 reforming (HMDP-SMR).

$$H_2 + S \leftrightarrow H_2S \; \Delta H^0_{298} \tag{1}$$

$$CH_4 + H_20 \leftrightarrow CO + 3H_2 \; \Delta H^0_{298} = 206kJ/mol \tag{2}$$

$$C0 + H_20 \leftrightarrow C0_2 + H_2 \; \Delta H^0_{298} = -41.2kJ/mol \tag{3}$$

$$CH_4 + 2H_20 \leftrightarrow C0_2 + 4H_2 \; \Delta H^0_{298} = 206kJ/mol \tag{4}$$

$$2CH_4 + H_20 + C0_2 \leftrightarrow CO + C0_2 + C_2H_2 + 4H_2 \; \Delta H^0_{298} \tag{5}$$

In contrast to SMR, Partial oxidation of methane (POM) and autothermal reforming (ATR) are other well-known technologies for producing H_2 and require the use of catalysts at higher operating pressure and temperature > 800°C. Transition metal catalysts such as Ni-based and Ni/C_eO_2 and noble metal catalysts are 2 types of POM metal-based catalysts [10]. A study by *Krummenacher, et al.* [11] reviewed that the noncatalytic process of producing H_2 through POM involves gasification of CH_4 and O_2 feed at a temperature ranging from 1300 - 1500°C and pressure between 3 - 8MPa. While ATR process is isothermal, and the reformer receives steam and O_2 for simultaneous reforming and oxidation reactions. Both POM and ATR use WGS and purification units to increase H_2 yield and convert CO to CO_2. Both processes cost more than competing ones

because of O_2 extraction from atmospheric air. Not long ago, membrane assisted autothermal reforming (MA-ATR) system has been suggested to reduce the cost of downstream purification units. In MA-ATR system, the use of the solid circulation of O_2 carrier, downstream WGS, and PSA units to prevent the mixture of H_2 from exiting CO_2 are not needed [12]. Nevertheless, high operational costs because of the use of ASU to extract O_2 and the high cost of noble metal-based catalysts; release of CO_2 emission into the environment are drawbacks of POM and ATR methods of H_2 generation. The overall efficiency of POM method is about 50% and both technologies cost more than SMR [13]. Hence, the use of thermal energy sources with the absence of greenhouse emissions to drive endothermic reforming and partial oxidation; improvement of overall efficiency of both POM and ATR technologies are needed urgently. Eqs (6) and (7) are chemical reactions of the POM process, while Eqs (8) and (9) represent chemical reactions of the ATR method.

$$CH_4 + \frac{1}{2}0_2 \leftrightarrow C0 + 2H_2 \ \Delta H_{298}^{0} = -36kJ/mol \tag{6}$$

$$C0 + H_20 \leftrightarrow C0_2 + H_2 \ \Delta H_{298}^{0} = -41.2kJ/mol \tag{7}$$

$$4CH_4 + 0_2 + 2H_20 \leftrightarrow 10H_2 + 4CO \ \Delta H_{298}^{0} = -71kJ/mol \tag{8}$$

$$C0 + H_20 \leftrightarrow C0_2 + H_2 \ \Delta H_{298}^{0} = -41.2kJ/mol \tag{9}$$

Unlike POM and ATR which required additional units to separate O_2 from air feed, sorption enhanced-chemical looping (SE-CL) involves both oxidation and reduction of oxygen carriers to produce synthetic gas. In contrast to sorption-enhanced steam methane reforming (SE-SMR) which also has been viewed as an alternative system to conventional SMR, the SE-CL approach allows the reuse and capture of CO_2 in H_2 generation plant [14][15]. The first stage of SE-CL involves a reaction of light hydrocarbon and solid specie with oxygen carrier (NiO) to produce synthetic gas and solid. The second react with CO_2 to enhance syngas production and regenerate the feed catalyst (NiO). While the third is an exothermic carbonation reaction to capture unprocessed CO_2. Added to that, the chemical looping waster splitting (CLWS) method of H_2 generation that exclude WGS, PSA and preferential oxidation (PROX) reaction has also been studied. The CLWS process involves the combustion of biofuel, H_2O disassociation and oxidation of air molecules [16][17]. The production of H_2 and CO_2 in different reactors for effective separation of H_2 from other by-products without the need for separation and purification units makes the process a promising one. On the contrary, NO_X and dioxins production because of the involvement of oxygen carriers during the combustion process is reported by *Hua & Wang*. [18]. Despite the advantages of chemical looping processes like increase in H_2 yield and CO_2 extraction and capture, fossil fuels burning to drive the endothermic reactions of first and second reactions; sorbent (CaO-based or MgO-based) decay after several chemical reactions because of sintering deactivation has been reported as drawbacks [19]. Nevertheless, *Erans, et al.* [20] suggested that the removal of sulphur from reacting feedstocks and the introduction of zirconium catalytic support can mitigate some of the above-mentioned drawbacks. Thus, carbon emissions associated with this technology can be prevented by incorporating a solar energy system and shift reactions. While required thermal energy for the calcination of $CaCO_3$ to produce CaO can be minimised by the adoption of the Calera method. Calera process of CO_2 capture involves feeding liquid calcium (Ca), magnesium (Mg), sodium (Na), chloride (Cl), hydroxide (OH) and O_2 as represented below in Eq 14 to form synthetic $CaCO_3$ and $MgCO_3$ [21]. Eqs (10 - 13) are chemical reactions of the SE-CL process.

$$CH_4 + NiO \leftrightarrow CO + 2H_2 + Ni \ \Delta H_{298}^{0} = 203kJ/mol \tag{10}$$

$$C0_2 + Ni \leftrightarrow NiO + CO \ \Delta H_{298}^{0} = 43kJ/mol \tag{11}$$

$$CaO + C0_2 \leftrightarrow CaCO_3 \ \Delta H_{298}^{0} = -179.8kJ/mol \tag{12}$$

$$MgO + C0_2 \leftrightarrow MgCO_3 \ \Delta H_{298}^{0} = -118kJ/mol \tag{13}$$

$$Wastewater/Brine \ (2CO_2 + Ca + Mg + 2Na^+ + Cl^- + O_2 + OH^-) \leftrightarrow CaCO_3 + MgCO_3 + NaOH + NaCl \tag{14}$$

Eqs 1 – 13 above are combinations of exothermic and endothermic reactions which states that heat is required to break chemical bonds and heat is also released when a product is formed. Enthalpy (ΔH) with positive signs is endothermic which means that external heat is needed for the reaction. While Enthalpy (ΔH) with negative signs is exothermic (release of heat when a product is formed). CH_4, H_2O and CO conversions, H_2 yield (%) and CO_2 capture efficiencies are represented in Eqs 15 – 18 below.

$$CH_4 \ and \ H_2O_{gas} \ conversion = \frac{n_{CH_4}^{01} - n_{CH_4}^{1}}{n_{CH_4}^{01}} = \frac{n_{H_2O}^{01} - n_{H_2O}^{1}}{n_{H_2O}^{01}} = \frac{n_{CO}^{1} - n_{CO}^{01}}{n_{CH_4}^{01}} = \frac{n_{H_2}^{1} - n_{H_2}^{01}}{3.n_{CH_4}^{01}} \tag{15}$$

$$CO \ conversion = \frac{n_{CO}^{02} - n_{CO}^{2}}{n_{CO}^{02}} = \frac{n_{H_2O}^{02} - n_{H_2O}^{2}}{n_{CO}^{02}} = \frac{n_{CO_2}^{2} - n_{CO_2}^{02}}{n_{CO}^{02}} = \frac{n_{H_2}^{2} - n_{H_2}^{02}}{n_{CO}^{02}} \tag{16}$$

$$H_2 \ yield \ (\%) = \frac{n_{H_{2,out}}}{n_{H_{2,in}}} x \ 100 \tag{17}$$

$$CO_2 \ capture = \frac{n_{CH_{4,in}} - n_{CH_{4,out}} - n_{CO_{2,in}} - n_{CO_{2,out}}}{n_{CH_{4,in}}} x \ 100\% \tag{18}$$

Distinct from photovoltaic (PV) technology, concentrating solar power (CSP) is more efficient in converting photon energy into electricity. In the CSP system, photon energy from the sun ray is absorbed by mirrors and transported to the solar furnace (receiver) in form of the heat exchanger and exchanged the absorbed heat with the working fluid. The absorbed thermal energy is utilised for electricity generation in a Rankine cycle. The introduction of thermal storage to enable the generation of electricity during cloud cover and after sunset makes the technology a promising one. On the contrary, *Boretti, et al.* [22] maintained that

CSP costs more than photovoltaics because of the high investment cost. Although, *Azouzoute, et al*. [23] assumed that the efficiency of the CSP system can be improved to recover the investment cost by installing it in MENA (the Middle East and North Africa) regions with more sunshine. For instance, a comparison of CSP in Spain and MENA countries shows that MENA countries achieved higher electricity production output and cost 33.9% cheaper than CSP in Spain [23]. Nevertheless, *Labordena, et al*. [24] quoted that transmission losses because of long-distance and poor electricity transmission lines may impact the transition from conventional fossil fuels to CSP systems in developing countries. Therefore, the improvement of electricity transmission lines to minimise losses and the incorporation of H_2 generation plants to recover investment costs can promote the transition to CSP systems in developing regions.

Consequently, greenhouse emissions into the atmosphere because of the burning of fossil fuels to drive endothermic decomposition of feedstocks to syngas concentration; emission of CO_2 by-products and reluctance in efficiencies improvement of H_2 generation technologies remain unsolved issues. To address some of these aforesaid drawbacks, this work aimed to develop integrated HR and SE-CL technologies which will reply on CSP to substitute fossil fuels burning in reformer and combustor furnaces. The goal of this work also includes energy recovery to boost the efficiency by using downstream feedstock and H_2O for syngas cooling. To achieve this goal, the below points are implemented in a process simulation to boost efficiencies as well as reduce carbon footprints in fossil fuel processes of H_2 production.

a) Integration of HR-SE-CL for efficiency improvement and carbon reuse and capture;
b) use of CSP to drive the endothermic reactions of HR-SE-CL with CH_4 gas as working fluid;
c) application of a Rankine cycle to generate electricity through recovered heat from reformer and reactor;
d) CO_2 by-product captured via Calera's suggestion.

The scope of this work focused on modelling and simulating existing SMR, POM, ATR, HMDP-SMR, and SE-CL processes of H_2 generation; modelling and simulating the CSP system coupled with integrated SMR SE-CL, POM SE-CL, and ATR SE-CL processes to mitigate drawbacks of current hydrocarbon reforming methods of H_2 generation. In addition, integrated systems of H_2 generation in a cleaner way tend to include a Rankine cycle with the use of recovered heat from combustors and reformers.

2.0 Material and Simulation Method

CH_4, H_2O, a portion of H_2 gas, air, NiO and CaO were chosen materials to simulate HR-SE-CL plants. CH_4 react with H_2O_{gas} in the reformer to produce syngas in SMR method. CH_4 combust with extracted O_2 from the ASU to produce syngas in POM system. While both H_2O_{gas} and O_2 reform and oxidised with CH_4 to produce synthetic gas in ATR plant. Syngas (CO) produced get converted to CO_2 in WGS and separated from H_2 in the PSA unit. As for the downstream unit which is SE-CL, CO_2 by-product from reforming processes react with NiO to produce more syngas. Followed by regeneration of NiO catalyst for more syngas production before capture of CO_2 by-product with CaO. Sulphur present in CH_4 feed was absorbed with portion of H_2 gas before reforming and oxidation to minimise catalyst failure. Recovered heat from the reformer and reactor through the applications of heat exchangers was used to operate downstream units. CSP plants drive the endothermic reactions of upstream units except for HMDP-SMR (hybrid microwave plasma, steam methane and CO_2 reforming). To study and implement HR-SE-CL systems in a process simulation, three primary case scenarios are involved.

- Case 1 is modelling and simulating conventional SMR, POM, ATR, HMDP-SMR, and SE-CL to provide deep understanding of integrated systems functionalities and compare H_2 to CO_2 yields with hybrid systems.
- Case 2 is modelling and simulating the CSP system to provide the required thermal energy that will drive endothermic reactions of HR-SE-CL processes of H_2 generation.
- Case 3 is modelling and simulating solar-driven integrated SMR-SE-CL, POM-SE-CL, and ATR-SE-CL processes of H_2 generation coupled with a Rankine cycle.

2.1 Modelling and Simulating Conventional SMR, POM, ATR, and SE-CL Methods of H_2 Generation.

Modelling of these technologies was carried out in Aspen Plus software and the Peng-Robinson equation of state was employed to predict the thermodynamic properties of some streams. The Ideal gas property method is used to accommodate a small deviation between low pressure and optimum temperature. System components are conventional and solid. While mixed is the only substream of the system. Assumptions taken into consideration for conventional and integrated systems of H_2 production are described below:

- Steady state condition for all processes.
- Heat duty estimates downstream activation energy because of heat and pressure losses.
- All feed operating parameters apart from flowrates are in mesophilic and thermophilic temperatures and atmospheric pressure.
- Input variables of reformer and combustor are based on results of parametric sensitivity analysis and literature.
- 3 bar operating pressure for all reformers and combustors.
- 0.21 oxygen, 0.78 nitrogen, and 0.1 argon mole fractions are the compositions of air fed to the system.

- Nickel oxide (NiO) is consumed in the first reaction and regenerated in the second reaction.
- Sulphur content in CH_4 gas is about 5% [25].
- H_2 yield of each conventional hydrocarbon reforming plant is multiplied by 8.8 to estimate the total carbon emission.
- H_2 yield of the SE-CL plant is multiplied by 8.8 and subtracted by captured by-CO_2 to estimate the total carbon emission.
- By-CO_2 from PSA unit of hydrocarbon reforming method is fed to SE-CL second reactor and integrated solar-driven H_2 generation technologies.
- Absence of deactivation during multiple desorption-reduction cycles.
- CH_4 gas combustion provided endothermic calcination of reactants in conventional reforming methods.

Fig. 1a shows a process flow diagram of the SMR process of H_2 generation described in Eqs 1 - 4. Pumps, heat exchangers (HEX), sulphur remover (absorber), heaters (including VAP), SMR reformer (Gibbs), WGS (HTS and LTS) reactors (stoichiometric), coolers, and PSA are primary components of this simulated plant. The SMR process of generating H_2 product start by feeding CH_4 into the heater to raise the temperature to 350°C and received by sulphur absorber unit where a portion of H_2 react with sulphur to form H_2S. The off-gas from the reformer is cooled by preheating the temperature of H_2O to 122 °C (saturated steam) in the HEX and received by the vaporiser for superheating. CH_4 without sulphur content react with H_2O_{gas} from the vaporiser in the SMR reformer to produce syngas (CO, H_2 and CH_4) prior entering the WGS unit. Reforming temperature and pressure are kept at 800°C and 3 bar. As the CO content is high, WGS reactors that uses CO catalytic converter converts the cooled product gases (CO and H_2O_{gas}) into CO_2 and H_2 (promotion of H_2 formation). PSA separate H_2 from CO_2 and other unreacted syngas. Process fuel from the PSA like unreacted CH_4 is re-entered into the reformer for more syngas generation.

A typical simplified flow diagram of HMDP-SMR of H_2 generation is depicted in Fig. 1b. The hybrid microwave plasma and SMR system as described in Eqs 1, 2, 3, and 5 accommodates the recycling of unprocessed exit syngas (CH_4 and CO_2). In the process simulation, steam reacts with desulphurised CH_4 in the microwave plasma source (MPS) to produce CO, CO_2, H_2 and C_2H_2($acetylene$). Unlike conventional SMR that utilises an external firing furnace within the reformer, the HMDP arc electrodes torch is powered by electricity. 807°C and 3 bar are kept as plasma reformer operating parameters to minimise difficulties in handling the optimum pressure and temperature and to prevent electrode erosion. The first separator ensures the exit of CO from other by-products. Thereafter, CO syngas enters the WGS for an exothermic reaction. H_2 and CO_2 from LTS are cooled, mixed with other synthetic gas, and flow to the PSA unit. In the PSA unit, H_2 and C_2H_2 are separated from other gases and stored. Whilst a portion of by-CO_2 is fed to the reformer. Electricity generation by a steam cycle is incorporated into the system to recover wasted heat because of a high degree of ionisation.

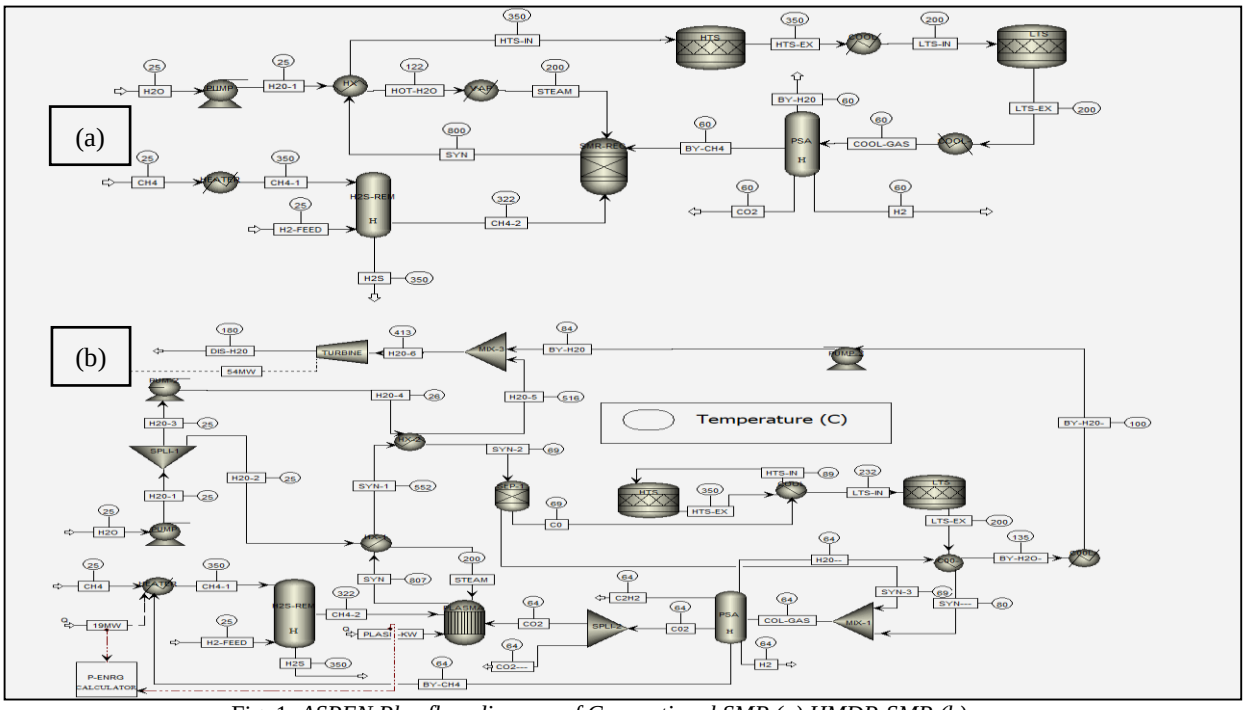

Fig. 1: *ASPEN Plus flow diagram of Conventional SMR (a) HMDP-SMR (b).*

As illustrated in Fig. 2a, the simulated POM model utilises an air separation unit (ASU) and combustor (Gibbs). Other POM components are the same as SMR. ASU receives the atmospheric air, O_2 is extracted, and enters into the combustor where partial oxidation of desulphurised $CH_{4\text{gas}}$ take place. Combustion temperature and pressure are kept at 800°C and 3 bar. Syngas (CO, H_2 and CH_4) from the combustor are cooled by raising the temperature of H_2O to 122 °C in the HEX. Vaporiser received saturated steam and turns it into steam. Next steps to convert CO and H_2O_{gas} into CO_2 and H_2, and separate both product gases from unreacted CH_4 and H_2O_{gas} have the same operating principle as SMR. Recovered CH_4 from the PSA is re-entered into

the CH_4 feed-heater for recycling. Fig. 2b presents a flow diagram of ATR system of H_2 generation. ATR process is a combination of SMR and POM. In the autothermal reformer, the adiabatic pre-reforming of $CH_{4\text{gas}}$ occurs in the presence of both oxidants (H_2O_{gas} and O_2) at temperature and pressure of 800°C and 3 bar. Unreacted CH_4 from the PSA is re-entered into the reformer. CO as one of the by-products is oxidised to CO_2 in shift reaction described in Eq 3. While recovered unreacted H_2O from the PSA unit mixes with steam from the vaporiser prior entering the reformer. Steam flowrate entering the reformer was controlled by the splitter because excess steam in the autothermal reformer will increase the amount of unoxidised O_2.

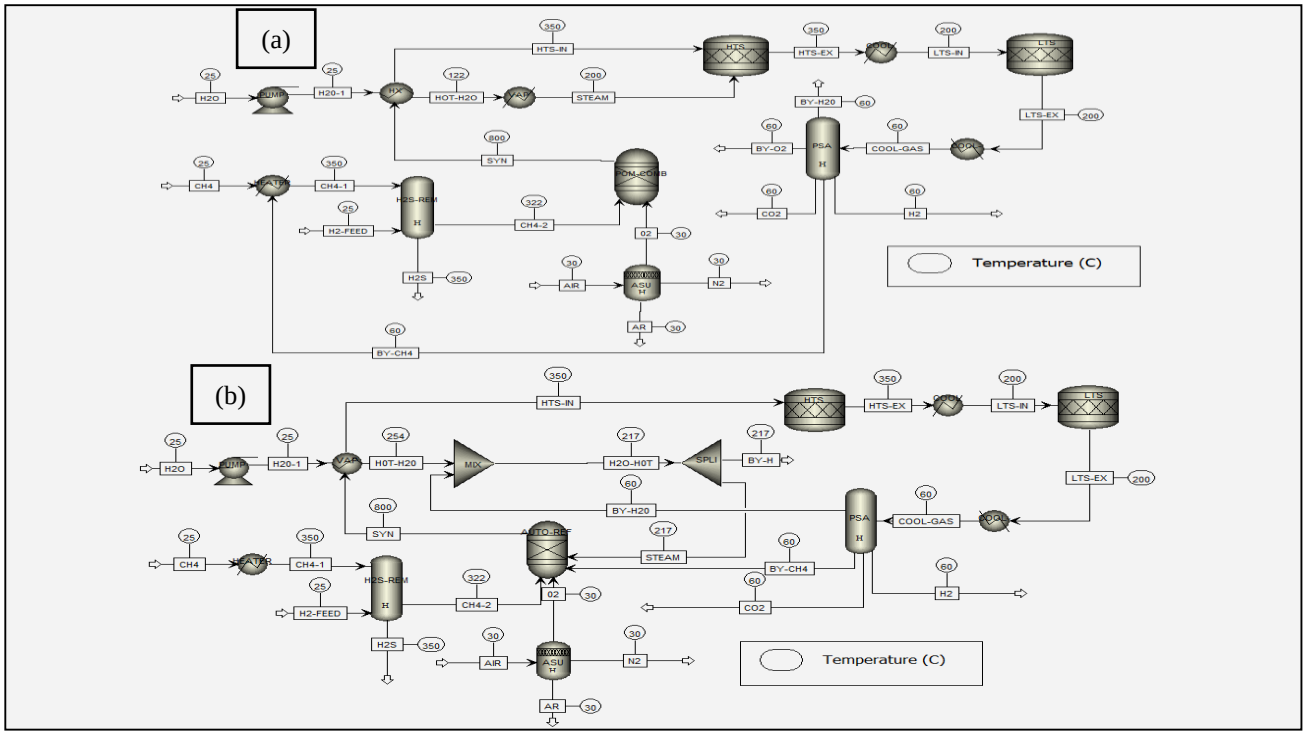

Fig. 2: *ASPEN Plus flow diagram of Conventional POM (a) Conventional ATR (b).*

A typical flow diagram of a sorption enhanced-chemical looping (SE-CL) which is illustrated in Eqs 10 – 12 is represented in Fig. 3a. In the process flow diagram, NiO as O_2 carrier reacts with desulphurised CH_4 in the first SE-CL reactor to produce CO, H_2 and Ni. The first separator allowed the exit of Ni prior entering the SE-CL second reactor. CO and H_2 from separator 1 enters WGS reactors where the chemical reaction described in Eq 3 occurs. Ni and by-CO_2 from the PSA unit react in the SE-CL second reactor to produce CO and NiO catalyst. The oxidation of CO from the SE-CL second reactor to CO_2 occurs in the shift reactors. Unconverted by-CO_2 is captured by the exothermic reaction of CaO to produce $CaCO_3$ as final product. To ensure that hydrocarbon reforming processes are entirely carbon emission-free by preventing the endothermic calcination of $CaCO_3$, the Calera process of CO_2 capture as written in Eq 14 is proposed and simulated. The process flow diagram displayed in Fig. 3b uses a chemical-equilibrium reactor and separator units. The feeds ($Ca, Mg, 2Na^+, Cl^-, O_2$ and OH^-) react with CO_2 under ambient and atmospheric conditions to produce $CaCO_3$, $MgCO_3$, $NaCl$ and $NaOH$. Produced $CaCO_3$ and $MgCO_3$ can be utilised in cement industries.

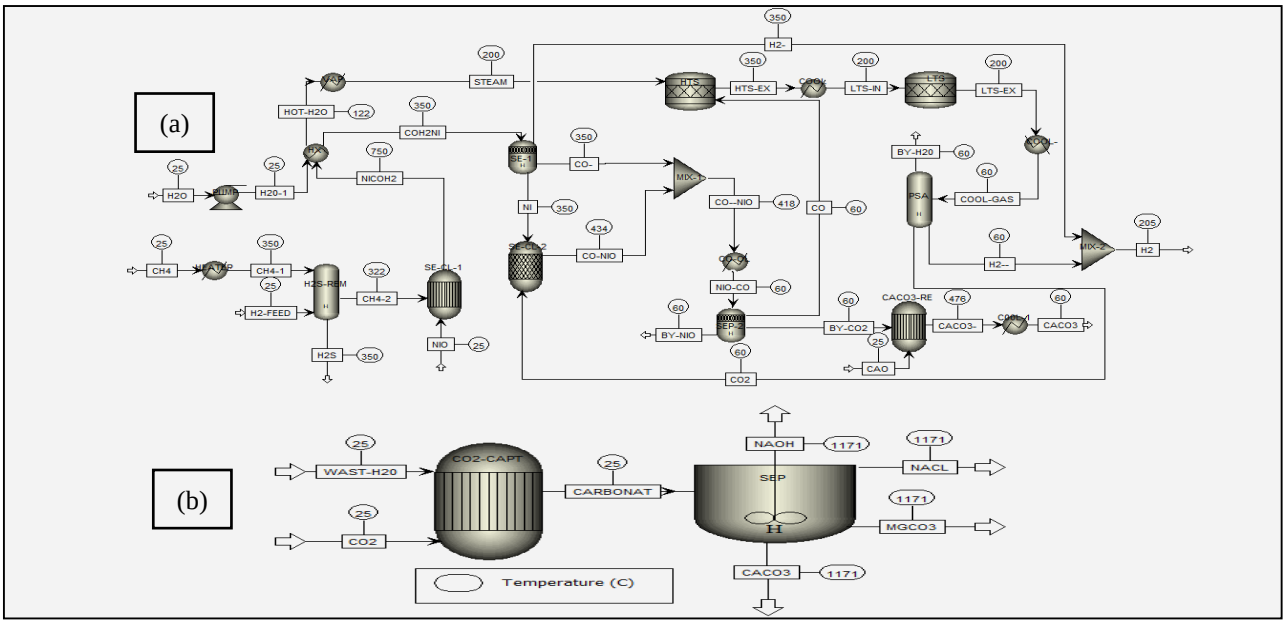

Fig. 3: *ASPEN Plus flow diagram of SE-CL with shift reactions (a) Calera process of CO_2 capture by wastewater/brine (b).*

2.2 Modelling and Simulation of Concentrating Solar Power System (CSPS)

The Modelling of CSPS was done in SAM-NREL (National Renewable Energy Laboratory) and MATLAB. The input parameters used for the simulation are shown in Table 1. As the integrated HR-SE-CL needs thermal energy from the CSP furnace for feedstock decomposition, the algorithm of the CSPS simulation from SAM was exported to MATLAB for modification and inclusion. Solar field parameters, collector, and receiver orientation of the CSP were simulated in the MATLAB environment and the results were saved in the MATLAB workspace for Simulink input.

Table 1. CSP plant specifications and configurations

Parameters	Value	Parameters	Value
Solar Field Parameters		**Solar Field Design Point and Land**	
Solar multiple	2.6	Actual number of loop	235-271
Design point DNI	$950W/m^2$	Total aperture reflective area	1233280m
Row spacing	15m	Solar field area	762 acres
Wind stow speed	$25m/s$	Total land area	10687 acres
HTP pump efficiency	0.85	Non-solar field land area multiplier	1.4
Number of field subsection	2	**Collector and Receiver**	
Heat Transfer Fluid and Collector Orientation		Reflective aperture area	$656m^2$
Loop intake HTF temperature	350°C	Aperture width, total structure	6m
Loop exit HTF temperature	750 - 1050°C	Length of collector assembly	115m
Freeze protection temperature	150°C	Number of modules per assembly	8
Min and max single flowrates	1 and $12kg/s$	Average surface-to-focus path length	2.15m
Design min header flow velocity	$2m/s$	Piping distance between assemblies	1m
Design max header flow velocity	$3m/s$	Absorber tube inner diameters	0.076m
Min and max field flow velocities	0.3 and $0.66m/s$	Absorber tube outer diameter	0.08m
Stow and deploy angles	170 and 10 degrees	Glass envelope inner and outer diameters	0.115 and 0.12
		Design min and max header flow velocities	2 and $3m/s$

2.3 Modelling and Simulating Solar-Driven Integrated SMR-SE-CL, POM-SE-CL, and ATR-SE-CL Processes of H_2 Generation Coupled with Rankine Cycle.

A flow diagram displayed in Fig. 4 represents an integrated process simulation of solar-driven SMR-SE-CL method coupled with a Rankine cycle. The integrated system consists of heat exchangers (HEX), reformers, and WGS reactors. $CH-1$ to $CH-10$ represent CH_4 flow streams. While H_2O-1 to H_2O-15 describe the flow of H_2O and steam streams. In the process simulation, CH_4 feed under ambient temperature exchange heat with hot CH_4 leaving the furnace to raise the temperature to 350°C and received by the sulphur remover unit. Pure CH_4 exiting the desulphurisation zone enters the furnace to increase the temperature to 1050°C and dropped to 800°C after leaving HEX-1. The second splitter (SPLI-2) which received hot CH_4 gas

from the first HEX split the gas into two. Some portion of hot CH_4 gas enters the SMR reformer where it reacts with steam from the vaporiser to produce syngas. Steam was generated by utilising H_2O to cool the exit hot syngas leaving the SMR reformer. The remaining process of producing H_2 and CO_2 and separating both via WGS and purification processes are the same as conventional SMR in Fig. 1a. While unreacted CH_4 from the SMR reformer mixes with CH_4 from second splitter (Spli-2) and reacts with NiO prior entering into the first reactor (SE-CL-1). Regeneration of NiO, feeding CO to WGS unit, separation of H_2 and CO_2 from other end products, and the reaction of CaO with by-CO_2 to form $CaC0_3$ are entirely the same as SE-CL in Fig. 3a. Heat recovered from reformers is utilised to generate steam for a Rankine cycle with pump and turbine discharged pressures of 221.2 and 10 bars. The use of a furnace (FURN) block in the Aspen model allowed temperature control of endothermic reactions that occurred in SMR and SE-CL reactors. The furnace block is assumed to be a CSP receiver furnace where activation energy and temperature can be adjusted. To make use of solar energy from the CSP system to replace the need for external firing within the reformer furnaces, the SMR-SE-CL Aspen model was transformed into flow driven dynamic model and called from the Simulink. Simulated CSP results saved in the MATLAB workspace like HTF intake and exit temperatures were then used as input variables for the Simulink model. In the Simulink environment, HTF intake and exit temperatures were connected to the SMR-SE-CL furnace and CH_4 gas is the working fluid of the integrated system. As the hybrid system requires an external energy source during initialisation, a portion of produced H_2 can substitutes fossil fuels burning. The integration of HEX for syngas cooling prior entering other units with lower operating temperatures made it possible for electricity generation and reduction of thermal energy demand for downstream units. Steam from cooling units (HEX) was utilised to drive a steam turbine with an efficiency of 0.72. Whereas electrically powered devices like pumps and PSA units can be powered by electricity generated from the steam cycle. Pumps operating in a steam cycle have an efficiency of 0.75.

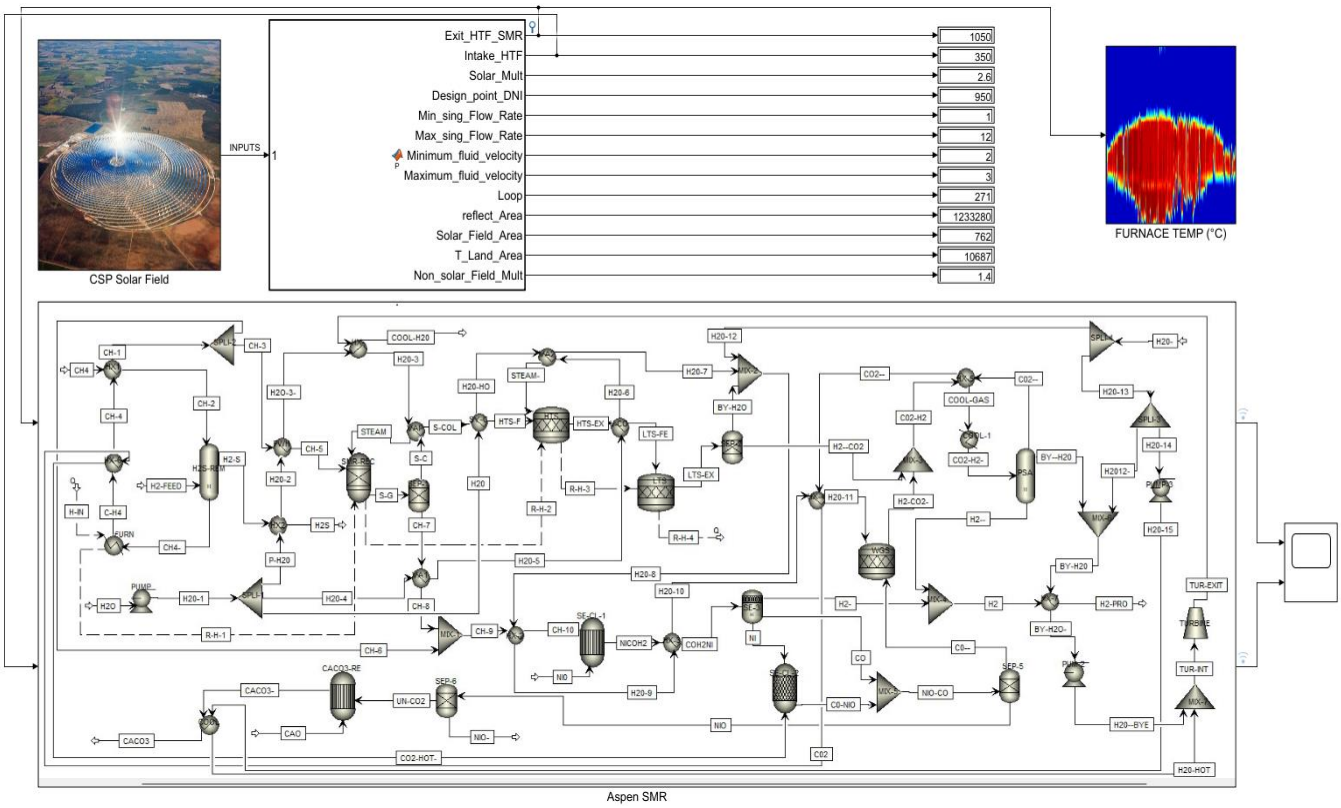

Fig. 4: *CSP-ASPEN Plus flow diagram of SMR-SE-CL.*

In contrast to an integrated SMR-SE-CL plant, the POM-SE-CL process requires less energy for feedstock decomposition. The integrated POM-SE-CL system consists of HEX, reformers, and WGS reactors. The representation of CH_4 and H_2O flow streams are entirely the same as SMR-SE-CL plant. Due to the exothermic nature of POM, heat recovered from syngas cooling prior entering and leaving the WGS unit was utilised for generating steam and raising the temperature of CH_4 flowing into the desulphurisation zone to 350°C. While additional thermal energy needed to operate upstream, and downstream units came from the CSP furnace. The process of extracting O_2 from air is the same as conventional POM. The exothermic reactions to increase H_2 yield and convert CO to CO_2 and separate both via shift reactions and purification processes are entirely the same as that of conventional POM. Regeneration of NiO catalyst, CO generation, CO feed to WGS unit, separation of H_2 from CO_2, and formation of $CaC0_3$ as one of the by-products are still the same as SE-CL plant. Like the SMR-SE-CL plant, recycled heat was used to power downstream units and to generate steam. A process flow diagram of an integrated solar-driven POM-SE-CL coupled with a steam cycle is shown in Fig. 5. The integration of CSP into POM-SE-CL coupled with the Rankine cycle is the same as the integrated solar-driven SMR-SE-CL system. The plant configuration of solar-driven ATR-SE-CL system coupled

with a Rankine cycle is very similar to solar-driven POM-SE-CL except for the use of both H_2O_{gas} and O_2 in the reformer as depicted in Fig. 6.

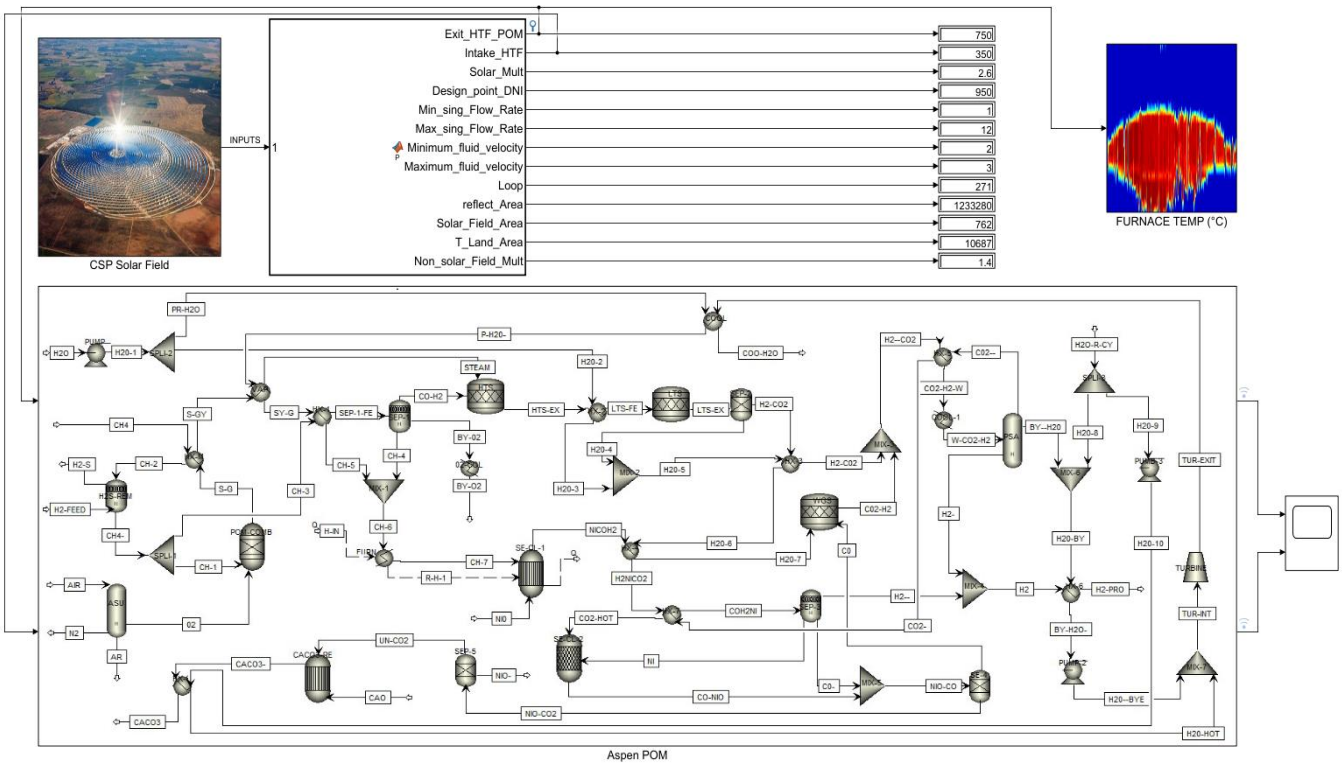

Fig. 5: *CSP-ASPEN Plus flow diagram of POM-SE-CL.*

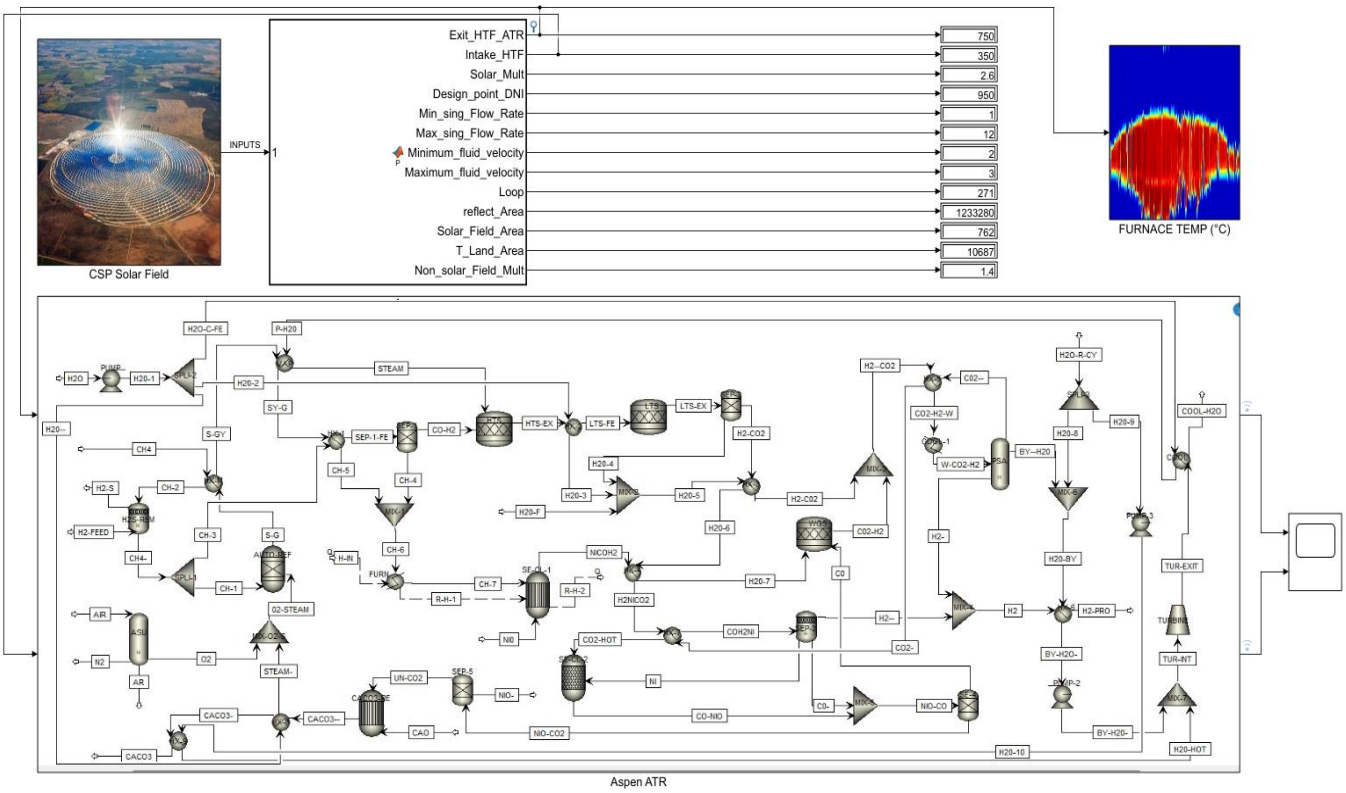

Fig. 6: *CSP-ASPEN Plus flow diagram of ATR-SE-CL*

3.0 Results and Discussion

As shown in Table 2, H_2 yields in SMR, HMDP-SMR, and SE-CL are higher compared to other methods. The high degree of ionisation in MPS and recycling of by-CO_2 in both HMDP-SMR and SE-CL led to high syngas concentration. H_2 concentration rate for POM was higher than ATR because of difficulties in balancing flowrates of both oxidising agents (O_2 and H_2O_{gas}) in the reformer. Thus, an equilibrium flowrate of O_2 and H_2O_{gas} in the ATR reformer is necessary to maximise the conversion efficiency of both reactants. Despite the exothermic nature of both POM and ATR processes of H_2 generation, heat is still

required to remove sulphur from CH_4 feed. HMDP-SMR seems to be eco-friendly technology because of the use of electricity to drive the endothermic decomposition of the reactants but higher activation energy in contrast to competing technologies limits the widespread of the system. FORTRAN calculation for the activation energy of HMDP-SMR indicates that the presence of by-CO_2 in the reformer increased electricity consumption making the system less efficient than conventional SMR. It was also observed that an increase of CO_2 flowrate at constant flowrates of other reactants (CH_4 and steam) accelerates the rate of unprocessed CO_2 by decreasing the H_2 volume concentration because of weak reaction discrepancy. The generation of C_2H_2 syngas in HMDP-SMR was very low due to the inability to recycle enough CO_2. The use of a high volume of H_2O for cooling the syngas leaving HMDP-SMR reformer allowed integration of steam cycle for electricity generation. The use of recovered thermal energy in the SE-CL system allowed the incorporation of shift reactions to produce more H_2 and convert CO to CO_2 from the first and second reactors. By-CO_2 (2591.6kg) capture and regeneration of sorbent (NiO) in the SE-CL method allowed high product purity and H_2 yield making the emerging technology a promising one. However, integrated SMR and SE-CL remain one of the cheapest methods of producing H_2 because of the high generation of syngas and the absence of ASU units.

Table 2: Feed, product and CO_2e results of conventional hydrocarbon reforming processes of H_2 generation.

Streams:	SMR		POM		ATR		HMDP-SMR		SE-CL	
CO_2e of each stream	Feed	Product	Feed	Product	Feed	Product	Feed	Product	Feed	Product
H_2O $(kmol/min)$ (kg/min)	129	0.625 11.3	65.6	0.6 13.3	45.2	0.6 13.3	600	471.6 8496.5	117.2	0.6 13.3
CH_4 $(kmol/min)$ (kg/min)	64.1		64.1		64.1		64.1		58.8	
Air $(kmol/min)$ (kg/min)			160		198					
O_2 $(kmol/min)$ (kg/min)			33.6	1.5 48.2	41.6 1330.5					
H_2 $(kmol/min)$ (kg/min)	3.3	256.8 517.6	3.3	192.6 388.2	3.3	173.6 349.9	3.3	256.7 517.6	3.3	235.6 474.8
CO_2 $(kmol/min)$ (kg/min)		64.2 2824.9		64.2 2824.9		64.2 2824.9	500 22004.9	64.2 2824.8	117.8 5183.3	58.9 2591.6
H_2s $(kmol/min)$ (kg/min)		3.2 109.4		3.2 109.4		3.2 109.4		3.2 109.4		3.2 109.4
C_2H_2 $(kmol/min)$ (kg/min)								6E-10 1.6E-08		
NiO $(kmol/min)$ (kg/min)									58.9 4398.3	58.9 4398.3
Ni $(kmol/min)$ (kg/min)									58.9 3456.1	
CaO $(kmol/min)$ (kg/min)									58.9 3302.3	
$CaC0_3$ $(kmol/min)$ (kg/min)										58.9 5893.9
H_2 to CO_2 ratio	4:1		3:1		2.7:1		4:1		4:1	
Carbon dioxide equivalent (CO_2e) in kg/min)	4554.88 (517.6*8.8)		3416.16 (388.2*8.8)		3079.12 (349.9*8.8)		4554.88 (517.6*8.8)		1586.64 [(474.8*8.8) - 2591.6]	

In CSP simulated result, it was observed that a temperature >800°C for exit loop heat transfer fluid (HTF) is unachievable in SAM process simulation but practical in MATLAB. A decrease in flow volume occurs each time the temperature of the outlet loop HTF is increased. Thus, keeping the same flow volume at the aforesaid temperature means an increase in solar multiple. However, more increase in solar multiple increases the fluid flowrate of the system leading to higher investment cost which includes the cost of additional land area and equipment. This show that downsizing the solar furnace is necessary to achieve optimum exit loop HTF temperature in an existing CSP (parabolic trough and tower). As listed in Table 3, the highest H_2 yield was achieved in SMR-SE-CL compared to POM-SE-CL and ATR-SE-CL processes. Nonetheless, the total energy required to operate the SMR-SE-CL method is enormous due to the endothermic nature of the system (reaction of CH_4 with steam, CH_4 with NiO, CO_2 with Ni). H_2 to CO_2 yield for both POM-SE-CL and ATR-SE-CL processes outperform conventional POM and ATR as recorded in Table 3. The data in Table 3 suggests that the integration of SE-CL into POM and ATR as a hybrid improved the efficiencies of both systems leading to high syngas concentration. While the application of thermal energy recovery enhanced the exergy efficiencies of all the integrated plants. The total required thermal energy during endothermic

reactions of each feedstock in the reformer and reactor was calculated by Aspen plus to estimate energy loss during each operation. The outcome of this work suggests that integration of HR-SE-CL into an existing CSP plant with some modification to accommodate CH_4 as the working fluid is possible by keeping the same operating parameters with lesser feed flowrates to reduce activation energy.

Table 3: Feed, product, EI, PO, heat duty, CO_2e and syngas ratio results of HR-SE-CL processes of H_2 generation.

Streams	SMR-SE-CL		POM-SE-CL		ATR-SE-CL	
	Feed	Product	Feed	Product	Feed	Product
H_2O $(kmol/min)$ (kg/min)	483.8	251.2 4525.95	428	259.6 4677	502.5	213.2 5642.2
CH_4 $(kmol/min)$ (kg/min)	122.1 2052		122.1 2052		122.1 2052	
Air $(kmol/min)$ (kg/min)			153		103	
O_2 $(kmol/min)$ (kg/min)			32.13		21.6	
H_2 $(kmol/min)$ (kg/min)	5.8	465.143 937.7	5.8	400.96 808.3	5.8	421.9 850.5
CO_2 $(kmol/min)$ (kg/min)		116.3 5117.7		116.3 5117.7		116.3 5117.7
H_2s $(kmol/min)$ (kg/min)		5.8 198.2		5.8 198.2		5.8 198.2
NiO $(kmol/min)$ (kg/min)	58.9 4398.3	58.9 4398.3	52.1 3891.3	52.1 3891.3	65.3 4875.5	65.3 4875.5
Ni $(kmol/min)$ (kg/min)	58.9 3456.1		52.1 3057.8		65.3 3831.1	
CaO $(kmol/min)$ (kg/min)	116.3 6521		116.3 6521		116.3 6521	
$CaC0_3$ $(kmol/min)$ (kg/min)		116.3 11638.7		116.3 11638.7		116.3 11638.7

Energy input (EI), power output (PO) and amount of carbon emission	SMR-SE-CL	POM-SE-CL	ATR-SE-CL
Activation energy for furnace (MW)	96.9	22.32	27.98
Heat duty (required thermal energy) of CH_4 + H_2O reformer due to loss (MW).	254.3		
Heat duty of CH_4 + $0.5O_2$ combustor due to loss (MW).		21.3	
Heat duty of CH_4 + O_2 + H_2O reformer due to loss (MW).			60.1
Heat duty of CH_4 + NiO reactor	253	223.8	280.4
Heat duty of $C0_2$ + Ni (MW)	54.9	86.5	61.1
Heat duty (other units "thermal and electrical") (MW)	80.3	45.7	53.4
Electricity output of turbine (MW)	5.3	5.42	10.24
Total energy requirement (MW)	734.1	394.2	472.74
H_2 to CO_2 ratio	4:1	3.5:1	3.6:1
Carbon dioxide equivalent (CO_2e) in kg/min)	Captured	Captured	Captured

3.1 Effect of reforming and combustion temperature and pressure

Parametric sensitivity analyses were carried out on conventional hydrocarbon reforming to study the effects of operating temperature and pressure on H_2 yield and purity as illustrated in Fig. 7. Temperature in the range of 400-900°C and pressure between 1-30 bars were used during the analysis to determine the variation of syngas composition. It was found that CH_4 and H_2O_{gas} conversion rates increased as the operating temperature increases leading to higher concentration and purity of H_2 and CO in SMR. On the contrary, an increase in SMR reformer pressure, decreases CH_4 and steam conversion rates, leading to lower syngas formation. The sensitivity analysis study of the reformer operating parameters (temperature and pressure) does follow Le Chatelier's principle which states that endothermic reaction is favoured by high temperature and low pressure [26]. Temperature and pressure effects on syngas formation for both POM and ATR follow the same trend as SMR during sensitivity analyses. However, O_2 oxidation to CO was not affected until the reaction temperature rose above 800°C because of the exothermic nature of POM process. Similarly, a shift to steam conversion in the ATR reformer due to a lack of unreacted O_2 was discovered. Nevertheless, excess O_2 in both POM and ATR reactors was neglected to prevent full oxidation and to allow more reaction of steam with CH_4 feed. High-purity syngas and reduction of activation energy by recycling unreacted CH_4 was feasible by keeping reformers and combustor temperature and pressure at 800°C and 3 bar. By taking advantage of recycling unreacted reactants, the need for reformers and combustor temperature and pressure optimisation were unimportant. As an increase in one of the reactant's ratios increases the activation energy leading to a decrease in the efficiency of the entire process, steam to carbon (S/C) ratio analysis was neglected. S/C ratio was substituted by employing chemical equations related to each process and use of equilibrium reactors. For example, *Fahim, et al.* [27] concluded that the overall S/C ratio of 4 (SMR and WGS) which is the industrial scale for SMR prevent the deposition of coke on the surface of the reformer catalyst. Nevertheless, *Chehade, et al.* [28] study shows that S/C ratio of 6 with the absence of shift reactors achieved the same H_2 concentration with industrial scale operating with WGS units. Syngas concentration at the SMR reformer exit gave a S/C ratio of 3:1. While 99.9% conversions efficiency of SMR feedstocks was reached. This was possible by recycling unprocessed feedstock and use of equilibrium and stochiometric reactors for reformer and WGS units. For this study, CH_4 and CO conversion efficiency follows similar trends reported by *Chehade, et al.* [28].

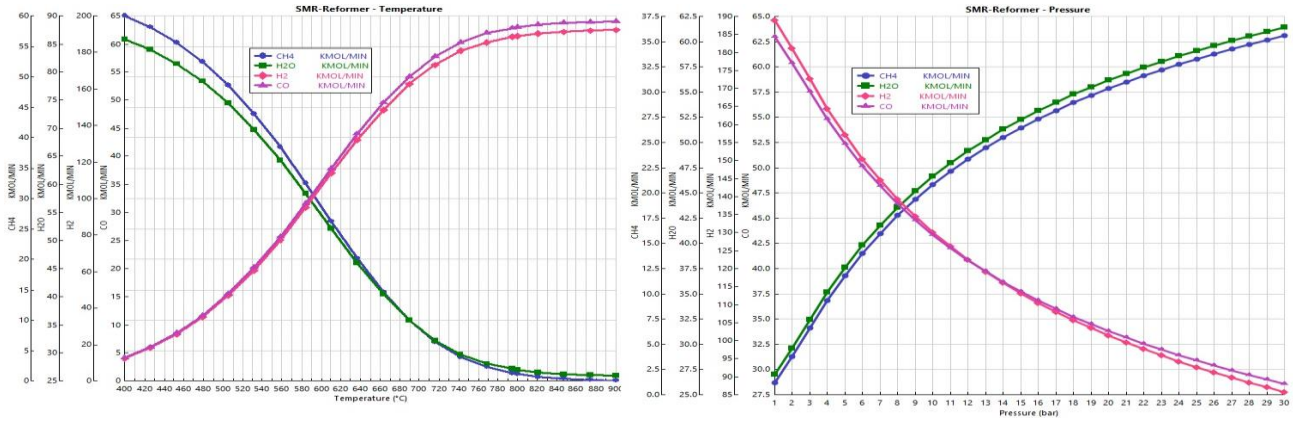

Fig. 7: *Temperature and pressure effects on H_2O_{gas} and CH_4 conversion to syngas for SMR.*

Effects of temperature and pressure on CH_4 and NiO, CO_2 and Ni conversion demonstrates that an increase in temperature increases the conversion rate of the reactants leading to high syngas concentration. From the parametric analysis study as displayed in Fig. 8, at a reforming temperature of 670°C, CH_4 and NiO achieved the highest syngas generation. Although, CH_4 with NiO reformer temperature was kept higher because of the endothermicity of the downstream reaction of CO_2 with Ni (utilisation of the exit heat from the SE-CL-1 reformer for NiO re-oxidation). Thus, the temperature effect of the reaction of CO_2 with Ni is more endothermic than the rest of the reactions. Further, it was observed that at a reaction temperature of 900°C, CO_2 and Ni could not achieve the maximum conversion rate. Between 400 - 500°C were CO_2 and Ni reaction temperature because an increase in temperature increases the amount of required heat leading to a high concentration of both CO and NiO. Operating pressure effects on syngas concentration are the same as other processes of H_2 generation. A ratio of 1 for NiO/C and Ni/C was adopted during the process simulation to eliminate the need for ratio effects analysis. This was achieved by employing equilibrium reactors that require a mass balance of reactants during the process simulations. In contrast to the endothermic reactions of the above-mentioned methods, temperature and pressure increase on CO_2 with CaO reaction do not enhance the formation of $CaCO_3$ because of the exothermic nature of the process. The effect of CaO/C ratio was neglected because with a ratio of 1, excess heat demand can be mitigated [29]. Molar extent was employed to control the flowrate of steam to syngas (H_2 and CO_2) in WGS because an increase in steam increases the amount of H_2 and CO_2 concentration due to the interaction between CO and H_2O. The effect of molar extent in WGS shows that both H_2 and CO_2 increased with the increase of both CO and H_2O_{gas} conversion rate until a maximum limit is reached.

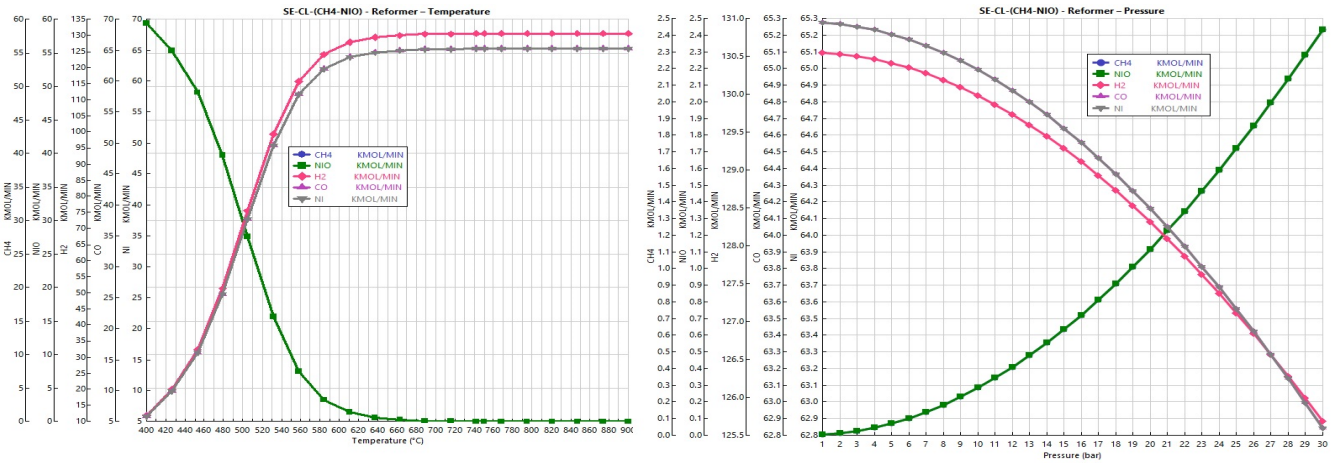

Fig. 8: *Temperature and pressure effects on CH_4 and NiO conversion to syngas and Ni for SE-CL.*

3.2 Model validation and Economic analysis

A comparison of SE-CL-SMR has been made to validate H_2 to CO_2 concentration with experimental data published by *Antzara, et al.* [30] as illustrated in Table 4. From the model validation table, the present study shows a similar trend with higher H_2 yield. Distinct from the pyrolysis of hydrocarbon processes, hydrocarbon reforming methods of H_2 production coupled with SE-CL requires less CH_4 feedstock. For instance, *Parkinson, et al.* [31] mentioned that an additional 300kta of CH_4 feed is required in pyrolysis of CH_4 to produce 200kta of H_2. About $1.89/kg was reported as H_2 selling price of CH_4 pyrolysis [31]. However, between $2.2/kg - $2.9/kg was also report as H_2 selling price for SMR-CCS plant [32]. Nonetheless, any of the simulated plants is expected to achieve lower H_2 selling price because of the integration of SE-CL which allow the transfer of oxygen from oxygen-carrier, CO_2 recycle and electricity generation with recovered thermal energy. For instance, by using downstream feedstocks for upstream syngas cooling prior entering the separation units, exergy destruction was minimal in contrast to conventional SMR, POM and ATR. Furthermore, a reduction of H_2 selling price of the integrated system is possible because of the rate at which CSP installation cost is declining and more CSP installation in MENA (the Middle East and North Africa) regions. For example, electricity from a CSP plant located in Dubai cost $0.07/kWh [33] in contrast to $0.14/kWh in China [34]. Further reduction of H_2 selling price may be expected during raining season as *Singh, et al*. [35] maintained that low ambient and module temperature increases CSP absorption efficiency.

The result of the simulated hybrid H_2 and electricity generation systems means that the integration of HR-SE-CL into existing CSP plants by replacing the working fluid with CH_4 gas and upgrading the exit HTF temperature up to 1050°C is feasible. The outcome of this present study has also shown that the adoption of the simulated HR-SE-CL technologies will reduce carbon footprints and H_2 selling price especially, in regions with high solar direct normal irradiance (DNI). To ensure that the simulated hybrid system is carbon emission-free, a portion of produced syngas (H_2) can be utilised as furnace combustion fuel if the operating temperature falls below design conditions. Overall, this present study achieved ≥ 9.5% exergy efficiency compared to similar hydrocarbon reforming systems operating at the same feed flowrate. While bellow followings are the advantages of the simulated systems over similar ones.

a) Use of light hydrocarbon feedstock from fossil fuel or renewable (biomass, food wastes and wastewater via anaerobic digestion). b) The use of solar as a thermal energy source for feedstock decomposition to produce syngas and electricity in a Raking cycle. c) The utilisation of recovered heat to reduce the activation energy of downstream units.

Table 4: Model validation

Operating parameters	This work	[30]
Reformers operating temperature	434 - 800°C	850 - 900°C
Reformer operating pressure	3 bar	1 - 4 atm
S/C ratio	3:1	3:1
S/CO ratio	1:1	
CaO/C ratio NiO/C ratio	1:1	0.8 - 1
NiO/CaO ratio Ni/C ratio	1:1	0.2–0.7
CaO/C ratio	1:1	
H_2 to CO_2/CO product in ratio	4:1	3.5:1.1

4.0 Conclusion

Solar-driven integrated hydrocarbon reforming and sorption enhanced-chemical looping (SE-CL) processes have been explored, modelled, and simulated as potential replacements for conventional hydrocarbon reforming methods of H_2 generation. The Aspen models consist of both conventional and integrated solar-driven HR-SE-CL of H_2 generation. SAM and MATLAB were used to develop and simulate a CSP system that provided thermal energy for the integrated systems. The simulated CSP result shows that an increase in HTF exit temperature decreases the flow volume of the working fluid. While merging of the CSP system into integrated HR-SE-CL of H_2 generation was carried out in the Simulink environment. The introduction of heat exchangers in the integrated systems enhanced the exergy efficiency up to 9.5% over conventional reforming processes of H_2 production. While an increase in temperature at low operating pressure increases syngas concentration except for the exothermic reaction of CO_2 with CaO. The recycle of unreacted feeds promoted syngas formation at operating temperatures ≤ 800°C. Whereas unreacted CO_2 capture by wastewater/brine (Ca, Mg, Na, O_2, OH, and Cl) to form synthetic $CaC0_3$ eliminates the need for thermodynamic calcination of natural $CaC0_3$ to recover CaO. This study has demonstrated that achieving carbon neutrality and efficiency improvements by integrating CSP and heat recovery units into HR-SE-CL H_2 generation plants are feasible.

CRediT authorship contribution statement

Linus Onwuemezie: Conceptualization, Methodology, Software, Validation, Formal analysis, Investigation, Writing – Original Draft. **Hamidreza Gohari Darabkhani:** Methodology, Software, Validation, Formal analysis, Investigation, Writing – Original Draft, Writing – Review & Editing, Supervision, Project administration **Mohammad Moghimi Ardekani:** Software, Validation, Formal analysis, Investigation, Writing – Original Draft, Writing – Review & Editing, Supervision.

Declaration of competing interest

The authors declare that they have no known competing financial interests or personal relationships that could have appeared to influence the work reported in this paper.

References

[1] R. Dhingra, S. Das and a. R. Kress, "Making progress towards more sustainable societies through lean and green initiatives," *Cleaner Production,* vol. 37, pp. 400 - 402, 2012.

[2] I. Staffell, D. Scamman, A. V. Abad, P. Balcombe, P. E. Dodds, P. Ekins, N. Shah and a. K. R. Ward, "The role of hydrogen and fuel cells in the global energy system," *Energy & Environmental Science,* no. 12, pp. 463-491, 2019.

[3] C.-H. Kim, J.-Y. Han, S. Kim, B. Lee, H. Lim, K.-Y. L. and a. S.-K. Ryi, "Hydrogen production by steam methane reforming in a membrane reactor equipped with a Pd composite membrane deposited on a porous stainless steel," *International Journal of Hydrogen Energy,* vol. 43, no. 15, pp. 7684 - 7692, 2018.

[4] C.-H. Kim, J.-Y. Han, H. Lim, D.-W. Kim and a. S.-K. Ryi, "Methane steam reforming in a membrane reactor using high-permeable and low-selective Pd-Ru membrane," *Korean Journal of Chemical Engineering,* vol. 34, p. 1260 – 1265, 2017.

[5] K. Bareiß, C. d. l. Rua, M. Möckl and a. T. Hamacher, "Life cycle assessment of hydrogen from proton exchange membrane water electrolysis in future energy systems," *Applied Energy,* vol. 237, pp. 862 - 872, 2019.

[6] V. Spallina, B. Marinello, F. Gallucci, M. Romano and a. M. V. S. Annaland, "Chemical looping reforming in packed-bed reactors: Modelling, experimental validation and large-scale reactor design," *Fuel Processing Technology,* vol. 156, pp. 156 - 170, 2017.

[7] J. Holladay, J. Hu, D. King and a. Y. Wang, "An overview of hydrogen production technologies," *Catalysis Today,* vol. 139, no. 4, pp. 244 - 260, 2009.

[8] L. Bromberg, D. R. Cohn, A. Rabinovich, C. O'Brie and a. S. Hochgreb, "Plasma Reforming of Methane," *Energy Fuels,* vol. 12, no. 1, pp. 11 - 18, 1998.

[9] D. Czylkowski, B. Hrycak, M. Jasiński, M. Dors and a. J. Mizeraczyk, "Microwave plasma-based method of hydrogen production via combined steam reforming of methane," *Energy,* vol. 113, pp. 653 - 661, 2016.

[10] A. I. Osman, "Catalytic Hydrogen Production from Methane Partial Oxidation: Mechanism and Kinetic Study," *Chemical Engineering & Technology,* vol. 43, pp. 1 - 8, 2020.

[11] J. J. Krummenacher, K. West and a. L. D. Schmidt, "Catalytic partial oxidation of higher hydrocarbons at millisecond contact times: Decane, hexadecane, and diesel fuel," *Journal of Catalysis,* vol. 2015, no. 2, pp. 332 - 343 , 2003.

[12] S. Cloete, M. N. Khan and a. S. Amini, "Economic assessment of membrane-assisted autothermal reforming for cost effective hydrogen production with CO2 capture," *International Journal of Hydrogen Energy,* vol. 44, no. 7, pp. 3492 - 3510, 2019.

[13] C. M. Kalamaras and a. A. M. Efstathiou, "Hydrogen Production Technologies: Current State and Future Developments," *Conference Papers in Energy,* vol. 203, pp. 1 - 11, 2013.

[14] M. R. a. P. Ramos, "H2 production with CO2 capture by sorption enhanced chemical-looping reforming using NiO as oxygen carrier and CaO as CO2 sorbent," *Fuel Processing Technology,* vol. 96, pp. 27 - 36, 2012.

[15] B. Dou, K. Wu, H. Zhang, B. Chen, H. Chen and a. Y. Xu, "Sorption-enhanced chemical looping steam reforming of glycerol with CO2 in-situ capture and utilization," *Chemical Engineering Journal,* vol. 452, no. 4, p. 139703, 2023.

[16] M. Luo, Y. Yi, S. Wang, Z. Wang, M. Du, J. Pan and a. Q. Wang, "Review of hydrogen production using chemical-looping technology," *Renewable and Sustainable Energy Reviews,* vol. 81, pp. 3186 - 3214, 2018.

[17] X. Hua, Y. Fan, Y. Wang, T. Fu, G. Fowler, D. Zhao and a. W. Wang, "The behaviour of multiple reaction fronts during iron (III) oxide reduction in a non-steady state packed bed for chemical looping water splitting," *Applied Energy,* vol. 193, pp. 96 - 111, 2017.

[18] X. Hua and a. W. Wang, "Chemical looping combustion: A new low-dioxin energy conversion technology," *Journal of Environmental Sciences,* vol. 32, pp. 135 - 145, 2015.

[19] L. Li, B. Jiang, D. Tang, Z. Zheng and a. C. Zhao, "Hydrogen Production from Chemical Looping Reforming of Ethanol Using Ni/CeO2 Nanorod Oxygen Carrier," *Catalysts,* vol. 8, p. 257, 2018.

[20] M. Erans, V. Manovic and a. E. J.Anthony, "Calcium looping sorbents for CO2 capture," *Applied Energy,* vol. 180, pp. 722 - 742, 2016.

[21] D. Shashiprabha and a. R. Rajapakse, "Cement Types, Composition, Uses and Advantages of Nanocement, Environmental Impact on Cement Production, and Possible Solutions," *Advances in Materials Science and Engineering,* vol. 2018, pp. 1-12, 2018.

[22] A. Boretti, J. Nayfeh and a. W. Al-Kouz, "Validation of SAM Modeling of Concentrated Solar Power Plants," *Energies* , vol. 13, p. 1949, 2020.

[23] A. Azouzoute, A. A. Merrouni and a. S. Touili, "Overview of the integration of CSP as an alternative energy source in the MENA region," *Energy Strategy Reviews,* vol. 9, p. 100493, 2020.

[24] M. Labordena, A. Patt, M. D. Bazilian, M. Howells and a. J. Lilliestam, "Impact of political and economic barriers for concentrating solar power in Sub-Saharan Africa," *Energy Policy,* vol. 102, pp. 72 - 72, 2017.

[25] A. E. Lutz, R. W. Bradshaw, L. Bromberg and a. A. Rabinovich, "Thermodynamic analysis of hydrogen production by partial oxidation reforming," *International Journal of Hydrogen Energy,* vol. 29, no. 8, pp. 809 - 816, 2004.

[26] H. L. Chatelier, "On a general statement of the laws of chemical equilibria," Gauthier-Villars, Paris , 1884.

[27] M. A. Fahim, T. A. Al-Sahhaf and a. A. Elkilani, Fundamentals of Petroleum Refining, Elsevier, 2010, pp. 285 - 302.

[28] A. M. E. H. Chehade, E. A. Daher, J. C. Assaf, B. Riachi and a. W. Hamd, "Simulation and optimization of hydrogen production by steam reforming of natural gas for refining and petrochemical demands in Lebanon," *International Journal of Hydrogen Energy,* vol. 45, no. 58, pp. 33235 - 33247, 2020.

[29] A. Antzara, E. Heracleous, D. B. Bukur and a. A. A. Lemonidou, "Thermodynamic Analysis of Hydrogen Production via Chemical Looping Steam Methane Reforming Coupled with in Situ CO2 Capture," *Energy Procedia,* vol. 63, pp. 6576 - 6589, 2014.

[30] A. Antzara, E. Heracleous, D. B. Bukur and a. A. A. Lemonidou, "Thermodynamic analysis of hydrogen production via chemical looping steam methane reforming coupled with in situ CO2 capture," *International Journal of Greenhouse Gas Control,* vol. 32, pp. 115 - 128, 2015.

[31] B. Parkinson, J. W. Matthews, T. B. McConnaughy, D. C. Upham and a. E. W. McFarland, "Techno-Economic Analysis of Methane Pyrolysis in Molten Metals: Decarbonizing Natural Gas," *Chemical Engineering & Technology,* vol. 40, no. 6, pp. 1022 - 1030, 2017.

[32] J. Riley, C. Atallah, R. Siriwardane and a. R. Stevens, "Technoeconomic analysis for hydrogen and carbon Co-Production via catalytic pyrolysis of methane," *International Journal of Hydrogen Energy,* pp. 1 - 21, 2021.

[33] Y. Xu, J. Pei, J. Yuan and a. G. Zhao, "Concentrated solar power: technology, economy analysis, and policy implications in China," *Environmental Science and Pollution Research,* vol. 29, p. 1324 – 1337, 2021.

[34] J. Lilliestam and a. R. Pitz-Paal, "Concentrating solar power for less than USD 0.07 per kWh: finally the breakthrough," *Renewable Energy Focus,* vol. 26, pp. 17 - 21, 2018.

[35] V. P. Singh, V. Vijay, G. S. H.a, D. K. Chaturvedi and a. N. Rajkumar, "Analysis of solar power variability due to seasonal variation and its forecasting for Jodhpur region using Artificial Neural Network," *CPRI,* vol. 9, no. 3, pp. 140 - 148, 2013.